Note added in proof: Since submission of this manuscript, we have directly identified p70. IL-2 was cross-linked to [^{3}H]mannose-labeled HUT-102B2 cells with a cleavable cross-linker, and 17A1 immunoprecipitates were subjected to electrophoresis on a two-dimensional nonreducing-reducing gel system. p70 was identified as a 65- to 77-kD doublet below the diagonal consistent with cleavage of a single IL-2 molecule.

REFERENCES AND NOTES

1. K. A. Smith, *Immunol. Rev.* **51**, 337 (1980).
2. R. J. Robb, A. Munck, K. A. Smith, *J. Exp. Med.* **154**, 1455 (1981); R. J. Robb, W. C. Greene, C. M. Rusk, *ibid.* **160**, 1126 (1984).
3. J. W. Lowenthal, R. H. Zubler, M. Nabholz, H. R. MacDonald, *Nature (London)* **315**, 669 (1985); T. Uchiyama *et al.*, *J. Clin. Invest.* 76, 446 (1985).
4. A. M. Weissman *et al.*, *Proc. Natl. Acad. Sci. U.S.A.* **83**, 1463 (1986); M. Fujii *et al.*, *J. Exp. Med.* **163**, 550 (1986).
5. T. Uchiyama, S. Broder, T. A. Waldmann, *J. Immunol.* **126**, 1393 (1981).
6. W. J. Leonard *et al.*, *Nature (London)* **300**, 267 (1982).
7. W. J. Leonard, J. M. Depper, R. J. Robb, T. A. Waldmann, W. C. Greene, *Proc. Natl. Acad. Sci. U.S.A.* **80**, 6957 (1983); W. J. Leonard *et al.*, *J. Biol. Chem.* **260**, 1872 (1985).
8. R. J. Robb and W. C. Greene, *J. Exp. Med.* **158**, 1332 (1983).
9. W. J. Leonard *et al.*, *Nature (London)* **311**, 626 (1984); T. Nikaido *et al.*, *ibid.*, p. 631; D. Cosman *et al.*, *ibid.* **312**, 768 (1984); J. Miller *et al.*, *J. Immunol.* **134**, 4212 (1985).
10. W. C. Greene *et al.*, *J. Exp. Med.* **162**, 363 (1985).
11. M. Hatakeyama *et al.*, *Nature (London)* **318**, 467 (1985); S. Kondo *et al.*, *ibid.* **320**, 75 (1986).
12. R. J. Robb, *Proc. Natl. Acad. Sci. U.S.A.* **83**, 3992 (1986).
13. P. F. Pilch and M. P. Czech, in *Molecular and Chemical Characterization of Membrane Receptors*, C. Venter *et al.*, Eds. (Liss, New York, 1984), pp. 161–175.
14. M. Sharon and W. J. Leonard, unpublished observations.
15. L. A. Rubin *et al.*, *Hybridoma* **4**, 91 (1985).
16. G. Ortega, R. J. Robb, E. M. Shevach, T. R. Malek, *J. Immunol.* **133**, 1970 (1984).
17. M. B. Brenner, I. S. Trowbridge, J. L. Strominger, *Cell* **40**, 183 (1985).
18. G. N. Pavlakis and D. H. Hamer, *Proc. Natl. Acad. Sci. U.S.A.* **80**, 397 (1983).
19. L. P. Turek *et al.*, *ibid.* **79**, 7914 (1982).
20. D. W. Cleveland, S. G. Fischer, M. W. Kirschner, U. K. Laemmli, *J. Biol. Chem.* **252**, 1102 (1977).

21. We thank J. Harford and A. Weissman, NIH, for valuable discussions, K. Perry for her excellent secretarial assistance, M. Popovic, NCI, for HUT-102B2 cells, F. Ruscetti, NCI, for MT-2 cells, P. Howley, NCI, for ID13 cells, T. A. Waldmann, NCI, for anti-Tac, and W. E. Biddison, NIH, and D. Nelson, NCI, for 7G7B6. Rabbit antiserum to bovine albumin was obtained from Cooper Biomedical, ^{125}I-labeled IL-2 was initially provided by P. Kilian, Hoffmann–La Roche, and later obtained from New England Nuclear. Unlabeled IL-2 was a gift of F. Khan, P. Kilian, and J. Jensen, Hoffmann–La Roche.

1 July 1986; accepted 23 September 1986

Curvilinear, Three-Dimensional Motion of Chromatin Domains and Nucleoli in Neuronal Interphase Nuclei

UMBERTO DE BONI AND ARLAN H. MINTZ

The term "nuclear rotation" refers to a motion of nucleoli within interphase nuclei of several cell types. No mechanism or function has been ascribed to this phenomenon, and it was unknown whether nuclear structures in addition to nucleoli participate in this motion. Moreover, it was unclear whether nuclear rotation occurs independent of concurrent motion of juxtanuclear cytoplasm. The work reported here presents quantitative evidence, for three-dimensional intranuclear, tandem motion of fluorescently labeled chromatin domains associated with nucleoli and those remote from nucleoli. The results show that such motion is curvilinear, that it is not restricted to nucleoli, and, moreover, that it occurs independently of motion of juxtanuclear, cytoplasmic structures. These results suggest that this motion represents karyoplasmic streaming and its function is to transpose to nuclear pores those chromatin domains actively transcribed.

MOTION OF NUCLEOLI IN INTERphase nuclei has traditionally been termed nuclear rotation (NR) (*1–6*). Initial, descriptive observations of rotary movements of nucleoli in nuclei of neurons (*7, 8*) were followed by quantitative analyses of NR in neurons by Pomerat *et al.* (*9*) and others (*10*). In nonneuronal cells, NR has been documented for human olfactory epithelial cells (*11*) and for several other cell types (*5, 12–15*). Results showed that rates of NR in cultured cells, defined by displacement of the nucleolus, range from 1 revolution per minute in olfactory epithelial cells to 1 revolution per hour and slower rates in cultured neurons. No mechanism or functional significance has been assigned to this phenomenon. Furthermore, it was not known whether subnuclear structures other than nucleoli participate in the observed motion and whether NR occurs independently of concurrent cytoplasmic movement.

We present here evidence for motion, in three dimensions, of DAPI (4,6-diamidino-2-phenylindole)–stained, fluorescent chromatin domains in tandem with nucleoli (Fig. 1), in interphase nuclei of dorsal root neurons (DRN) in vitro. Further, we present evidence that such motion occurs independently of concurrent motion of cytoplasmic structures, including those in close proximity to the outer nuclear membrane.

Linear displacements of nucleoli in DRN, derived from measurements of displacement of phase-dark nucleoli and analyzed in a two-dimensional (2-D) plane, occur at mean rates of 0.077 ± 0.003 μm/min (± SEM; n = 269; range, 0 to 0.39 μm/min), which correspond to mean apparent angles subtended at the center of spherical nuclei of 0.746 ± 0.03 deg/min (with a range of 0 to 4.8 deg/min).

Observation of NR on time-lapse cine film shows that phase-dense granules, distributed throughout the nucleus, clearly move in tandem with nucleoli. To verify that these granules represent nuclear domains, and to quantify their motion, we used DAPI to vitally stain nuclei. We measured the location of intranuclear domains in seven neuronal nuclei, typically at intervals of 15 to 30 minutes, over periods from 120 to 420 minutes. The dynamics of nucleoli and DAPI-stained chromatin domains were essentially identical. For example, in the nucleus shown in Fig. 1, the nucleolus, one

Table 1. Comparison among representative translocation rates (T) and rotation rates (R) of nucleoli and of DAPI-stained fluorescent, nucleolus-associated and nonnucleolus-associated chromatin domains. Note absence of significant differences in rates (ANOVA, $P > 0.05$). Means ± SEM; n = 6.

Nucleolus		DAPI-stained domains			
		Nucleolus associated		Nonnucleolus associated	
T (μm/min)	R (deg/min)	T (μm/min)	R (deg/min)	T (μm/min)	R (deg/min)
2-D planar assay					
0.065 ± 0.01	0.608 ± 0.12	0.097 ± 0.03	0.823 ± 0.31	0.093 ± 0.01	0.910 ± 0.13
3-D dot-product assay					
0.093 ± 0.01	1.632 ± 0.27	0.070 ± 0.01	1.872 ± 0.30	0.070 ± 0.01	1.825 ± 0.16

Department of Physiology, University of Toronto, Toronto, Ontario, Canada M5S 1A8.

nucleolus-associated DAPI-stained domain, and one DAPI-stained domain clearly remote from the nucleolus, moved at mean rates of 0.065 ± 0.01, 0.097 ± 0.03, and 0.093 ± 0.01 μm/min, respectively, with rates of movement of these three structures not differing significantly [$n = 6$; by analysis of variance (ANOVA), $P > 0.05$]. Identical results were obtained for six additional, individually analyzed nuclei, with analyses of pooled data showing no significant differences (ANOVA, $P > 0.05$) in rates of translocation for nucleoli ($n = 71$ intervals) and DAPI-stained domains ($n = 66$ intervals). Whereas this observation is not surprising for nucleolar satellite DNA, it was also found to apply to fluorescent structures remote from nucleoli (Figs. 1, 2, and 3).

Conclusive interpretation of 2-D views of events occurring in three-dimensional (3-D), spherical structures, such as nuclei of the cells used here, is difficult. Moreover, in nuclei displaying two or more nucleoli, eclipses of the latter are common, indicating 3-D motion of karyoplasm. To more fully define the relations between movement of nucleoli and nonnucleolar fluorescent intranuclear domains, we measured their motion in 3-D (Fig. 3 and Table 1).

Dot-product vector analyses indicated that mean angles between vectors were not significantly different for nucleoli and fluorescent domains, regardless of whether the latter were located remote from or associated with nucleoli (Figs. 2 and 3 and Table 1). In the nucleus shown in Fig. 1, the nucleolus was shown to move with a mean vector angle of 1.63 ± 0.27 deg/min, whereas the nucleolus-associated and the nonnucleolus-associated DAPI-stained domains moved at 1.87 ± 0.30 and 1.83 ± 0.16 deg/min, respectively (ANOVA, $P > 0.05$). Data from a total of four such experiments and including five nucleoli, one nucleolus-associated and four nonnucleolus-associated DAPI-stained domains, indicated that their mean vector angles of 1.39 ± 0.22, 1.87 ± 0.30, and 1.82 ± 0.46 deg/min, respectively, did not differ significantly (Table 1), confirming the data from analyses in two dimensions.

To determine if concurrent motion of the cytoplasm accompanies NR, we kept phase-dense, cytoplasmic structures, located in the immediate juxtanuclear zone, in continuous focus throughout several experiments. While the nucleus under observation exhibited significant displacement of the nucleolus and of DAPI-fluorescent domains, such cytoplasmic structures were found to remain stationary. In one example (Fig. 4), the nucleolus moved through a planar angle of 100 degrees over a 30-minute interval (a mean 3-D vector angle of 2.61 ± 0.49 deg/min), with the cytoplasmic structure remaining stationary.

Our results indicate that NR is not restricted to motion of nucleoli, that it includes additional chromatin domains, and that it occurs independently of concurrent motion of cytoplasmic, juxtanuclear structures. Specifically, nucleoli and DAPI-stained, fluorescent chromatin domains moved along curvilinear trajectories that may have extended throughout the nucleus. While this motion was perceived as rotation when analyzed in a 2-D plane (as shown by the projection points onto the midnuclear parallelogram in Fig. 3 and demonstrated in Figs. 1 and 4), it represents, in reality, translocations of these structures in three dimensions. Three-dimensional analyses showed that the position of these structures extended, as a function of time, several micrometers above and below the midnuclear plane, at times approaching, although never exceeding, the length of the nuclear radius. Movements may be saltatory, with periods when the structures remain stationary and periods when they reverse direction (Figs. 3 and 4). Moreover, nucleoli may show precession, that is, rotation about their axis, as they move through the karyoplasm. As a result, fluorescent domains associated with the periphery of nucleoli, the nucleolar satellites, may assume different positions within the nuclear space, although they remain intimately associated with nucleoli (Fig. 3).

The moving fluorescent domains may represent loci of reversibly condensing and decondensing regions along chromatin fibers, rather than a physical translocation of a relatively permanent, structural domain. However, the close correlation of the rates of displacement of the fluorescent domains with that of nucleoli, which are structurally defined intranuclear organelles, makes this unlikely.

Given then that some nuclear structures are indeed in motion, conceptual difficulties

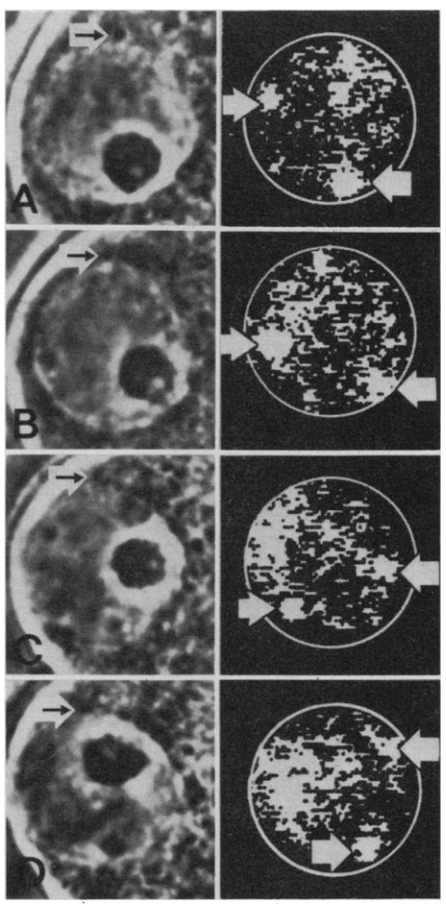

Fig. 1. Tandem motion of nucleolus (phase contrast, left column) and DAPI-stained fluorescent domains (digitally enhanced, right column), simultaneously analyzed (40-minute intervals). Of the two DAPI-stained domains identified (white arrows), one (A, lower right) is clearly associated with the nucleolar domain, while the other occupies a position remote from the nucleolus (A, upper left). Tandem motion also involves a larger, diffusely fluorescent chromatin domain, located at a nuclear edge opposite the labeled structures. Arrows in phase micrographs (left column, A to D) identify a juxtanuclear, cytoplasmic structure kept in focus during the entire experiment. Note that it remained stationary while nucleoli and DAPI-stained domains moved significantly. Neurons were dissociated from DRN ganglia of newborn mice (15 minutes, 0.25% trypsin, in Hanks balanced salt solution) and seeded into medium [90% Eagle's minimum essential medium, Hanks salts, 10% fetal bovine serum, glucose (600 mg/100 ml), nerve growth factor (100 ng/ml)] in collagen-coated, Bionique (Corning) Rose-type chambers. Cultures were maintained at 37 °C, in air, without carbon dioxide, on the stage of an inverted microscope (Nikon) with phase and fluorescence optics, photographic and video port. For DAPI fluorescence (25 μg/ml, final concentration), ultraviolet (UV) flux was reduced with neutral-density filters (Nikon, ND 16 + ND 32), permitting spatial analyses of domains without damage to cells, but requiring a silicon intensifier target video camera (RCA) for visualization. Control experiments over 5 days showed absence of an effect on viability of either DAPI or UV exposure. The microscope focus control, calibrated in micrometers, was used to continually follow and determine the vertical, spatial position of nucleoli and of fluorescent structures within the spherical nucleus. The position of nucleoli and fluorescent structures in the horizontal *xy*-plane was derived from measuring their position with respect to the nuclear center, derived from an optical section through the maximal diameter of the spherical nucleus. Video signals were enhanced after time-lapse capture by the "frame grabber" of a video processor board (Videtics, Canada), in an IBM-XT computer with hard disk. For analyses of the spatial position of intranuclear structures by a digitizer tablet and for representation, processed images along with a digitally stored calibration graticule were photographed either from the video monitor or from dot-matrix–printed hard copy.

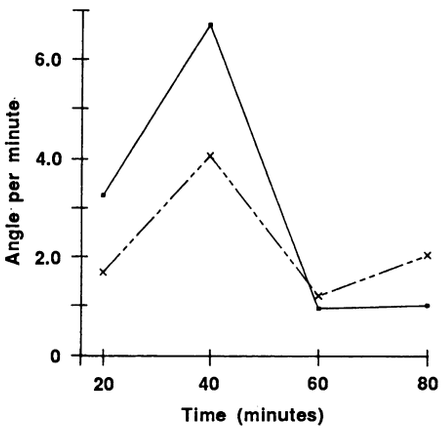

Fig. 2. Representative rates of spatial motion, in degrees per minute, of nucleolus (solid line) and DAPI-fluorescent domain (dashed line), the latter remote from the nucleolus, showing the tandem nature of movement. Angles were calculated as subtended at the center of the spherical nucleus, by 3-D dot-product vector analysis from the x, y, and z positions of the relevant structure. Values (x and y) were derived from measurements in the image plane; z value was from calibrated focus control on microscope.

arise in the consideration of the location of the interface between the moving and stationary components of this streaming of neuronal karyoplasm. Albrecht-Buehler (*15*) concluded that NR in his system, which differed from ours in that cycling rather than noncycling cells were examined, was related to events associated with mitosis. However, as shown here for neurons of cells developmentally arrested in interphase, events associated with mitosis are not a requirement for NR. Albrecht-Buehler (*15*) identified three loci as possible interfaces at which sliding movement associated with NR may occur: between the inner and outer membranes of the nuclear envelope, along the inner membrane of the nuclear envelope, or along the outer nuclear membrane.

The large number of nuclear pores, up to 18 per square micrometer of the membrane in cells of cerebral cortex (*16*), makes it unlikely that movement occurs between the two membranes comprising the nuclear envelope; moreover, this movement is unlikely because of the presence of fibrils of the stable intermediate-size class, which have been shown to extend, through the nuclear pores, from cytoplasm into karyoplasm (*17, 18*). Sliding along the interface between the peripheral surface of the nuclear lamina and the inner nuclear membrane is also unlikely, since specific structural proteins have been shown to intimately join the lamina to the inner membrane (*19, 20*). It is also improbable that a sliding interface exists between the outer nuclear membrane and the cytoplasm, since many cell types, including neurons, exhibit intermediate filaments that anchor the cytoskeleton to the nuclear membrane (*21–23*). Moreover, it is known that the outer nuclear membrane is continuous with that of the endoplasmic reticulum (*24*). Finally, we have observed that juxtanuclear, cytoplasmic structures, located within fractions of micrometers of the outer nuclear membrane, remain stationary when chromatin can be clearly shown to be in motion (Figs. 1 and 4), excluding significant motion of the outer nuclear membrane, often continuous with membranes of the endoplasmic reticulum (*24*).

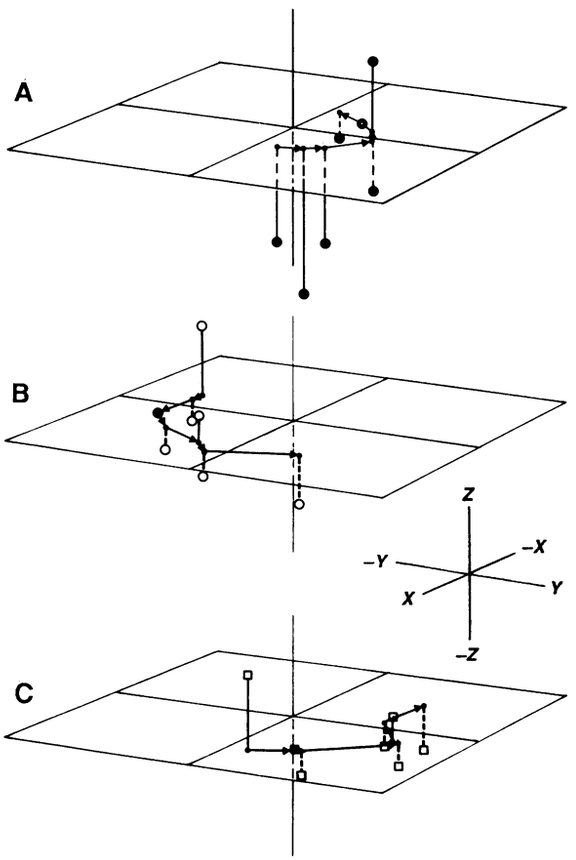

Fig. 3. Three-dimensional plot of trajectories of centers of nucleolus (A), nonnucleolus-associated (B) and nucleolus-associated (C), DAPI-stained fluorescent domains, of the nucleus shown in Fig. 1. Each structure is shown separately to facilitate visualization. Parallelogram represents horizontal, midnuclear plane with arrows connecting measured positions in xy-plane. z-Coordinates are indicated by symbols attached to vertical line. Filled symbols, without vertical lines, indicate that the structure lies in the horizontal, midnuclear plane. Note saltatory rate, pronounced motion in the z direction above and below the xy-plane, and counterclockwise motion, common to all three structures. Rotation of nucleolus on its own axis (precession) is indicated by the trajectory of the nucleolus-associated domain (C) differing to some extent from that of the nucleolus (A), indicated by "tumbling" of the fluorescent, nucleolar satellite about the periphery of the nucleolus.

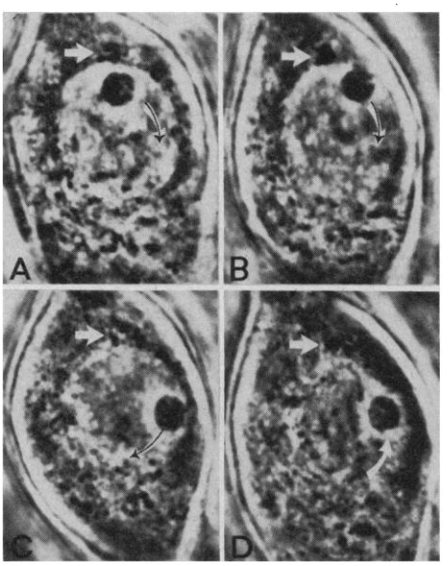

Fig. 4. Example of stationary, juxtanuclear, phase-dark cytoplasmic structure (white, straight arrows), continually maintained in focus, while nucleus "rotates" through 100 planar degrees in 45 minutes, (curved arrows). Note reversal of direction in (D). Interval between frames, 15 minutes. "Compromise" focus simultaneously visualizes the identified cytoplasmic structure, the nucleolus, and the nuclear envelope, resulting in an apparent, not real, change in morphology of the cytoplasmic structure identified.

We propose that the observed motion of karyoplasm represents the nuclear analog to cytoplasmic streaming, namely, "karyoplasmic streaming." We further propose that this streaming involves the fluid bilayer of the inner nuclear membrane (*25*), "flowing" around spatially fixed pore complexes, a flow envisioned to include nuclear lamina, nuclear matrix, and associated chromatin (*26*). In summary, we propose that this movement is functionally related to the intranuclear presence of contractile proteins, such as a specific species of intranuclear actin (*27–30*) or is related to the intermediate-size filaments recently identified in the nuclear envelope (*31*). While the work presented here was carried out in neurons, NR is not restricted to this cell type, and we speculate that the function of "karyoplasmic streaming" is to transpose to nuclear pores those chromatin domains actively transcribed. This hypothesis is supported by evidence for a

close association of actively transcribed genes with nuclear domains near the nuclear envelope (*32*) and is highly consistent with recent theoretical considerations of a defined 3-D structure of the cellular genome, specifically gated to a set of nuclear pores (*18*).

REFERENCES AND NOTES

1. W. Bloom, quoted in C. M. Pomerat, *Exp. Cell Res.* **5**, 191 (1953).
2. G. O. Gey, quoted in *ibid.*, p. 191.
3. F. E. Lehmann, *Exp. Cell Res. Suppl.* **6**, 16 (1958).
4. M. Girbardt, in *Aspects of Cell Motility*, P. L. Miller, Ed. (Cambridge Univ. Press, Cambridge, 1968), pp. 249–265.
5. C. A. Bourgeois, D. Hemon, C. Beaure D'Augeres, R. Robineaux, M. Bouteille, *Biol. Cell* **40**, 229 (1981).
6. F. Bard, C. A. Bourgeois, D. Costagliola, M. Bouteille, *ibid.* **54**, 135 (1985).
7. D. P. Murnaghan, *Anat. Rec.* **81**, 183 (1941).
8. J. Nakai, *Am. J. Anat.* **99**, 81 (1956).
9. C. M. Pomerat, W. J. Hendelman, C. Raiborn, J. F. Massey, in *The Neuron*, H. Hyden, Ed. (Elsevier, New York, 1967), pp. 119–173.
10. Z. Lodin, J. Booher, F. H. Kasten, *Exp. Cell Res.* **60**, 27 (1970).
11. C. M. Pomerat, *ibid.* **5**, 191 (1953).
12. V. Leone, T. C. Hsu, C. M. Pomerat, *Z. Zellforsch. Mikrosk. Anat.* **41**, 481 (1955).
13. E. Z. Hintzsche, *ibid.* **43**, 526 (1956).
14. C. R. Capers, *J. Biophys. Biochem. Cytol.* **7**, 559 (1960).
15. G. Albrecht-Buehler, *Cancer Cells (Cold Spring Harbor)* **1**, 87 (1984).
16. Z. Lodin, J. Blumajer, V. Mares, *Acta Histochem.* **63**, 74 (1978).
17. G. G. Maul, in *The Nuclear Envelope and the Nuclear Matrix*, G. G. Maul, Ed., vol. 2 of Wistar Symposium Series, Philadelphia, PA, 27–29 September 1981 (Liss, New York, 1982), pp. 1–11.
18. G. Blobel, *Proc. Natl. Acad. Sci. U.S.A.* **82**, 8527 (1985).
19. L. Gerace and G. Blobel, *Cell* **19**, 277 (1980).
20. ———, *Cold Spring Harbor Symp. Quant. Biol.* **46**, 967 (1982).
21. J. C. R. Jones, A. E. Goldman, P. M. Steinert, S. Yuspa, R. D. Goldman, *Cell Motil.* **2**, 197 (1982).
22. R. D. Goldman *et al.*, *Ann. N.Y. Acad. Sci.* **455**, *Intermediate Filaments*, 1 (1985).
23. J. Metuzals and W. E. Mushynski, *J. Cell Biol.* **61**, 701 (1974).
24. Electron micrographs of the neurons used in this study show clearly that the perinuclear space, between inner and outer nuclear membranes, is extensively continuous with channels of the endoplasmic reticulum intimately connecting the outer nuclear membrane to the membranes of the cytoplasmic reticulum and Nissl bodies.
25. N. M. Green, *Nature (London)* **297**, 287 (1982).
26. R. Hancock and T. Boulikas, *Int. Rev. Cytol.* **79**, 165 (1982).
27. A. Forer, in *Nuclear Division in the Fungi*, I. B. Heath, Ed. (Academic Press, New York, 1978), pp. 21–88.
28. T. G. Clark and J. L. Rosenbaum, *Cell* **18**, 1101 (1979).
29. J. W. Bremer, H. Busch, L. C. Yeoman, *Biochemistry* **20**, 2013 (1981).
30. H. Nakayasu and K. Ueda, *Cell Struct. Funct.* **10**, 305 (1985).
31. F. D. McKeon, M. W. Kirschner, D. Caput, *Nature (London)* **319**, 463 (1986).
32. N. Hutchison and H. Weintraub, *Cell* **43**, 471 (1985).

33. We thank K. Norwich for assistance with computer graphics for the 3-D image analyses and V. Kalnins and D. Van der Kooy for criticism of the manuscript. Supported by the Medical Research Council and the Natural Sciences and Engineering Research Council of Canada. U.D.B. was supported by an associateship of the Ontario Mental Health Foundation.

20 May 1986; accepted 2 September 1986

Chromosomal Localization of Muscle Nicotinic Acetylcholine Receptor Genes in the Mouse

ODILE HEIDMANN, ANDRÉS BUONANNO, BRIGITTE GEOFFROY, BENOÎT ROBERT, JEAN-LOUIS GUÉNET, JOHN P. MERLIE, JEAN-PIERRE CHANGEUX

The chromosomal localization of the genes encoding the four subunits of muscle nicotinic receptor was determined by analyzing restriction fragment length polymorphisms between two mouse species *Mus musculus domesticus* (DBA/2) and *Mus spretus* (SPE). Analysis of the progeny of the interspecies mouse backcross (DBA/2 × SPE) × DBA/2 showed that the α-subunit gene cosegregates with the α-cardiac actin gene on chromosome 17, that the β-subunit gene is located on chromosome 11, and that the γ- and δ-subunit genes cosegregate and are located on chromosome 1.

THE NICOTINIC ACETYLCHOLINE receptor (AChR) from fish electric organ and vertebrate skeletal muscle is a transmembrane protein composed of four different subunits synthesized from independent messenger RNA's (mRNA's) (*1*) and assembled into an $\alpha_2\beta\gamma\delta$ pentamer (*2*). Molecular cloning and nucleotide sequencing of complementary DNA (cDNA) and genomic sequences for the four genes from different species have disclosed a high degree of conservation of the protein structure throughout vertebrate evolution. Extensive homologies between subunits have suggested that the genes evolved by successive duplication of a common ancestor gene, with a first branch point for the α and β subunits and a second one for the γ and δ subunits (*3, 4*). Recently, Nef *et al.* (*5*) showed that, in the chick, the γ- and δ-subunit genes are separated by only 740 bp on the chromosome, and Shibahara *et al.* (*6*) isolated human genomic clones that hybridize to both the γ- and δ-subunit cDNA probes, thus suggesting a clustering of the AChR genes and a possible common control of their transcription.

We have made use of restriction fragment length polymorphisms (RFLP's) between two mouse species (*7*) to determine the chromosomal localization of the genes encoding AChR subunits and found that the four genes are not clustered in a single region but are distributed on three different chromosomes. The α-subunit gene cosegregates with the α-cardiac actin gene previously allocated to chromosome 17 by Czosnek *et al.* (*8*), the β-subunit gene is located on chromosome 11, and the γ- and δ-subunit

O. Heidmann, B. Geoffroy, J.-P. Changeux, Unité de Neurobiologie Moléculaire, Institut Pasteur, 25 rue du Docteur Roux, 75724 Paris, Cedex 15, France.
A. Buonanno and J. P. Merlie, Department of Pharmacology, Washington University School of Medicine, St. Louis, MO 63110.
B. Robert, Unité de Biochimie, Institut Pasteur, 75724 Paris, Cedex 15, France.
J.-L. Guénet, Unité de Génétique des Mammifères, Institut Pasteur, 75724 Paris, Cedex 15, France.

Table 1. Segregation of the AChR subunit genes and other known chromosomal markers in the 42 offspring of the DBA/2 × (DBA/2 × SPE) backcross. Results of genomic blots for the AChR subunit genes are reported as (−) when mice are homozygous for the DBA/2 allele and as (+) when mice are heterozygous for the DBA/2 and SPE alleles. ND, not determined. MHC_F and $MLC1_F/MLC3_F$

Locus	1	2	3	4	5	6	7	8	9	10	11	12	13	14	15	16
Chromosome 17																
Glo-1	+	−	+	−	ND	−	−	+	+	+	−	+	+	−	+	−
α-Cardiac actin	+	−	−	−	+	−	+	−	+	−	+	+	−	+	+	+
α-Chain AChR	−	−	−	−	+	+	+	−	+	−	+	−	+	+	+	+
Chromosome 11																
MHC_F	−	+	+	−	+	−	+	−	+	+	+	+	+	−	−	+
β-Chain AChR	−	+	+	−	+	−	+	−	+	+	+	+	+	−	−	+
Chromosome 1																
Idh-1	−	+	+	+	+	−	−	−	−	+	+	−	−	+	+	+
$MLC1_F/MLC3_F$	−	+	+	+	+	−	−	−	−	+	+	−	−	+	+	+
γ-Chain AChR	−	+	+	+	+	−	−	−	−	+	+	−	−	−	−	+
δ-Chain AChR	−	+	+	+	+	−	−	−	−	+	+	−	−	−	−	+